# Level-Set Based Carotid Artery Segmentation for Stenosis Grading

C.M. van Bemmel*, L.J. Spreeuwers, M.A. Viergever, W.J. Niessen

Image Sciences Institute, Room E 01.334, University Medical Center Utrecht,
Heidelberglaan 100, 3584 CX Utrecht, The Netherlands
{kees,luuk,max,wiro}@isi.uu.nl

**Abstract.** A semi-automated method is presented for the determination of the degree of stenosis of the internal carotid artery (ICA) in 3D contrast-enhanced (CE) MR angiograms. Hereto, we determined the central vessel axis (CA), which subsequently is used as an initialization for a level-set based segmentation of the stenosed carotid artery. The degree of stenosis is determined by calculating the average diameters of cross-sectional planes along the CA. For twelve ICAs the degree of stenosis was determined and correlated with the scores of two experts (NASCET criterion). The Spearman's correlation coefficient for the proposed method was 0.96 ($p<0.001$), versus 0.89 and 0.88 ($p<0.001$) for the manual scores, and a smaller bias and tighter confidence bounds for the automated method were found.

## 1 Introduction

Stroke is the third leading cause of death in the western world and is responsible for major disability among survivors [1]. Intra-arterial digital subtraction angiography (IA-DSA) has historically been regarded as the gold standard for visualization of the internal carotid artery (ICA). Especially the degree of stenosis is an important measure for selecting patients for carotid endarterectomy [2]. However, IA-DSA carries a risk of stroke in patients with atherosclerosis. Clinical studies have demonstrated that less invasive techniques, like magnetic resonance angiography (MRA) and computerized tomographic angiography (CTA), are useful alternatives for patient selection [3, 4].

Therefore, there is an interest in automated reproducible stenosis grading of carotid arteries from CT and MR data. Westenberg *et al.* performed vessel-diameter measurements on Maximum Intensity Projections (MIPs) of Gadolinium (Gd) Contrast-Enhanced (CE) MRA datasets along a line drawn perpendicular to the vessel [5]. Frangi *et al.* used a method in which a surface represented by a B-spline was fitted to the data using prior knowledge of the image formation process [6]. In this paper an alternative approach is adopted for semi-automatic segmentation of the ICA. First, a path-tracking tool is utilized, which automatically determines the central vessel axis (CA) of a stenosed carotid artery,

* This work is funded by Philips Medical Systems, Best, The Netherlands.

T. Dohi and R. Kikinis (Eds.): MICCAI 2002, LNCS 2489, pp. 36–43, 2002.

based on user-defined points. Subsequently, the stenosed artery is segmented using level-set techniques with the CA as initialization. The segmentation is used to determine the degree of stenosis. Previously, Lorigo *et al.* [7] presented level-set techniques for vessel segmentation. However, in this approach the CA is not used as initialization, which is an essential step in our approach. Moreover, the method has not been applied or evaluated to (carotid artery) stenosis grading. The technique presented in this paper was compared to manual scores on CE-MRA datasets and DSA images of twelve stenosed carotid arteries.

## 2 Method

The presented method segments the ICA using level-set techniques with the CA a collection of seedpoints. Figure 1 shows a block-diagram outlining the key steps in our approach. First, a method is applied that determines the CA (Section 2.1). Subsequently, the CA is used as initialization for level-set based segmentation of the ICA (Section 2.2). Finally, the vessel quantification is described in Section 2.3.

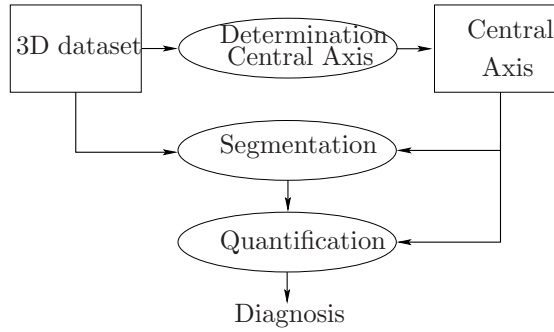


**Fig. 1.** Overall block diagram of the proposed method.

### 2.1 Central Axis Determination

The CA is determined as the minimum-cost path between two user-defined points [8]. Costs are given by the reciprocal value of an image in which vessel-like structures are enhanced, using the vesselness filter as described by Frangi *et al.* [9] (see also Section 2.2). A bi-directional search-tree is started from both the starting node and the goal node simultaneously. The evolution of the search tree is continued until the two fronts meet. The accuracy of the CA with respect to manual tracings has been demonstrated in [10].

### 2.2 Level-Set Based Vessel Segmentation

In this section we describe the level-set technique, as formulated by Osher [11] and Sethian [12], applied to segmentation of the ICA, with the CA as initialization. This segmentation can be regarded as the evolution of a front, or interface,

towards the vessel boundaries. Rather than evolving an interface itself, it is represented by the zero level-set of a higher dimensional function. To formalize these notions, let $\Gamma(t)$ denote a time-dependent closed 2-dimensional surface representing the evolving segmentation. This interface evolves in its normal direction according to:

$$\Gamma_t(t) = F \cdot \boldsymbol{N}. \tag{1}$$

Here $F$ denotes the speed function and $\boldsymbol{N}$ is the normal vector to the surface, pointing outwards. Now, a 3-dimensional function $\phi(t)$ is defined such that $[(\phi(t) = 0)] = \Gamma(t)$, *i.e.* $\Gamma(t)$ is represented by the zero level-set of $\phi(t)$ at all times. It can easily be shown that if $\Gamma(t)$ evolves according to Equation 1, the evolution of $\phi(t)$ is given by:

$$\phi_t(t) + F|\nabla\phi(t)| = 0. \tag{2}$$

Thus, the evolution of the zero level-set of $\phi(t)$ equals the evolution of $\Gamma(t)$. Therefore, in level-set based image segmentation, the evolution of $\Gamma(t)$ is implicitly defined by evolving $\phi(t)$. This approach has the advantage that topological changes in $\Gamma(t)$ (like breaking and merging) are handled naturally.

In order to capture the vessel boundaries, an appropriate speed function $F$ needs to be selected. For this purpose we investigated the effect of grey-level-, gradient- and vesselness-based speed functions.

1. *Grey-level based speed function*
   The histogram of the CE-MRA dataset shows two distinct peaks, representing the background and the vasculature. Therefore, two normal distributions were fitted on the histogram of the dataset. The parameters that describe the distribution of both the background and the vasculature ($\mathcal{N}(\mu_b, \sigma_b)$ and $\mathcal{N}(\mu_v, \sigma_v)$, respectively) were determined using the expectation-maximization algorithm [13]. Since in CE-MR angiography vessels give higher signal than the background, it is clear that $\mu_v > \mu_b$. Based on these parameters, the grey-level-based speed term is defined as:

$$F_I(x) = \frac{1}{\sigma_v\sqrt{2\pi}} \sum_{i=0}^{x} e^{-\frac{1}{2}(\frac{i-\mu_v}{\sigma_v})^2}, \tag{3}$$

   where $x$ is the image grey-value. Note that with this approach no ad hoc threshold parameter is selected as it is derived from image information.

2. *Gradient-level based speed function*
   The gradient image is calculated by convolving the dataset with the first-order derivative of the Gaussian kernel. The gradient-based speed function is given by:

$$F_\nabla(x) = \frac{1}{1 + \nabla I(x, \sigma_{grad})} \tag{4}$$

   where $\nabla I(x, \sigma_{grad})$ is the gradient computed at scale $\sigma_{grad}$ at position $x$.

3. *Vesselness-based speed function*
This speed term, $F_{\mathcal{V}}$, equals the vesselness function as described in [9], and is based on the eigenvalues $|\lambda_1| \leq |\lambda_2| \leq |\lambda_3|$ of the Hessian matrix, that is determined by convolving the image with the second order derivatives of the Gaussian kernel at scale $\sigma$. In case of an ideal tubular structure $|\lambda_1| = 0$, $|\lambda_1| \ll |\lambda_2|$, and $\lambda_2 = \lambda_3$. Moreover, the total magnitude of the eigenvalues reflects the amount of second-order structureness. Therefore, from the eigenvalues, three terms are constructed which are used in the vesselness filter, viz.:

$$\mathcal{R}_A \triangleq \frac{|\lambda_2|}{|\lambda_3|} \quad , \quad \mathcal{R}_B \triangleq \frac{|\lambda_1|}{\sqrt{|\lambda_2\lambda_3|}} \quad \text{, and} \quad \mathcal{S} \triangleq \|\mathcal{H}\|_F = \sqrt{\sum_j \lambda_j^2}.$$

Here $\mathcal{R}_A$ is essential for distinguishing between plate-like and line-like structures, $\mathcal{R}_B$ accounts for the deviation from a blob-like structure, and $\mathcal{S}$ is the measure of second-order structureness. In the ideal situation $|\lambda_1| = 0$, $|\lambda_1| \ll |\lambda_2|$, and $\lambda_2 = \lambda_3$. The vesselness-based speed function is a discriminant function based on these three terms:

$$F_{\mathcal{V}}(x) \triangleq \max_{\sigma_{min} \leq \sigma \leq \sigma_{max}} \begin{cases} 0 & \text{if } \lambda_2 > 0 \text{ or } \lambda_3 > 0, \\ v(x,\sigma) & \text{otherwise,} \end{cases} \tag{5}$$

where

$$v(x,\sigma) = (1 - e^{-\frac{\mathcal{R}_A{}^2}{2\alpha^2}}) e^{-\frac{\mathcal{R}_B{}^2}{2\beta^2}} (1 - e^{-\frac{\mathcal{S}^2}{2\gamma^2}}) \ . \tag{5a}$$

The parameters $\alpha$, $\beta$, and $\gamma$ tune the sensitivity of the filter to deviations in $\mathcal{R}_A$, $\mathcal{R}_B$, and $\mathcal{S}$, respectively. The filter is applied at multiple scales that span the expected vessel-widths.

4. *Combined speed function*
Since the speed terms mentioned above have different properties, a combined speed function can be composed by multiplying them:

$$F = F_I \ F_\nabla \ F_{\mathcal{V}}, \tag{6}$$

where a speed term is set to 1 if it is not included. All speed terms are normalized, so values are in the range $[0, 1]$.

### 2.3 Vessel Quantification

The degree of stenosis according to the NASCET criterion [2] is given by (see also Figure 2):

$$(1 - \frac{\text{Minimal Residual Lumen}}{\text{Distal ICA Lumen Diameter}}) \cdot 100\%. \tag{7}$$

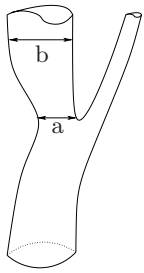


This measure is defined for DSA data, which are projection images. In the method we propose, the degree of stenosis is determined from cross-sectional MR slices. In order to determine the degree of stenosis that is comparable to the NASCET criterion, we used the average diameter of the cross-sectional planes along the CA. In this study 12 stenosed carotids arteries were screened. From all carotid arteries both a DSA dataset (consisting of three projections (posteroanterior, oblique, and lateral)) and a CE-MRA dataset were available.

**Fig. 2.** Schematic view of the linear lumen reduction measuring method according to the NASCET stenosis-criterion ($(1 - \frac{a}{b}) * 100\%$) used for the internal carotid artery.

## 3 Results

### 3.1 Central Axis Determination

In order to determine the CA, the vesselness image is computed at 25 scales (exponentially increasing) in the range of $\sigma$ = 0.25 - 7.5 mm. For the vessel-enhancement, the parameters $\alpha$ and $\beta$ were both fixed at 0.5, while $\gamma$ equals 25% of the maximum occurring pixel value in the 3D dataset. In case one of the eigenvalues is large, $\mathcal{S}$ will be large; the output of this filtering process is rather insensitive to the value of $\gamma$. In all datasets, the CA was everywhere located inside the lumen and could be used as initialization for the level-set based segmentation.

### 3.2 Level-Set Based Vessel Segmentation

Vessel segmentation is achieved via level-set techniques using the CA as initialization. Hereto, we implemented Equation 2 using a simple Euler forward-scheme with time-step $\Delta t = 0.1$. We tested the influence of the different speed functions as given by Equations 3 through 6 separately. The gradient-based speed image was computed using $\sigma_{grad} = 0.75$ mm, which is a trade-off between noise-suppression on the one side, and taking the width of the ICA into account on the other side. The parameters of the vesselness-based speed image were equal to those used for the CA determination (see Section 3.1). It was found that the segmentation was most robustly estimated using a combination of the speed terms. Therefore, the evaluation on all datasets was carried out by evolving a front utilizing the CA as initialization and the speed function given by $F = F_I \; F_\nabla \; F_\mathcal{V}$. In Figure 3 a typical segmentation and a diameter-vs-length plot are shown.

### 3.3 Stenosis Grading

Expert grading of the DSA images was performed by averaging the scores from all available projections without vessel over-projection. Quantification of CE-MR angiograms was done by two experts by averaging the degree of stenosis

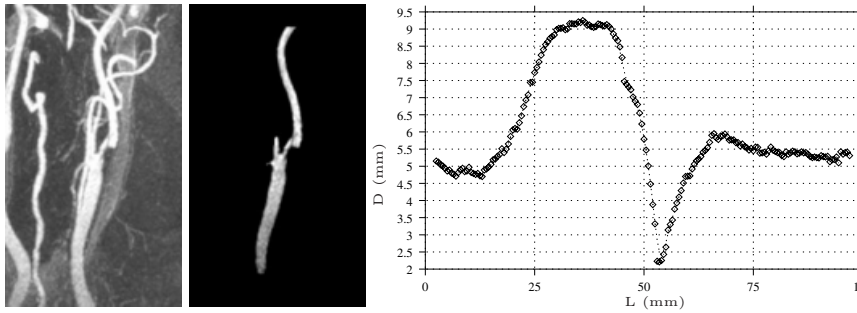


**Fig. 3.** Maximum Intensity Projections (MIP) of a 3D CE-MR angiogram of the ICA (left) with corresponding segmentation (middle) and diameter-vs-length plot (right) from which the stenosis grade can be determined.

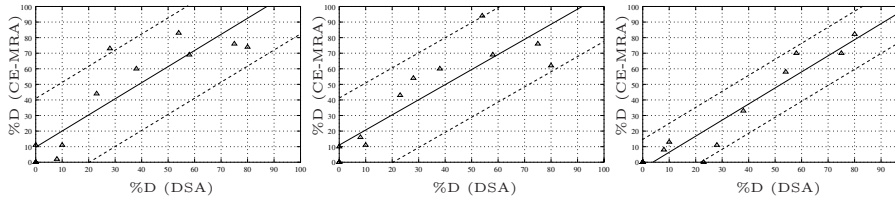


**Fig. 4.** CE-MRA vs DSA. Degree of stenosis is measured in 12 carotid arteries. Linear regression expert I (left), expert II (middle), and level-set based technique (right). Dashed lines indicate 95% confidence. It can be observed that the semi-automatic method better correlates with the gold standard provided by DSA. Moreover, the bias introduced by the method is smaller and the confidence bounds are tighter.

computed from MIPs in posteroaterior, oblique, and lateral views without vessel over-projection. The same ICAs were graded with the level-set based technique by determining the average diameter of cross-sectional planes along the CA, that was resampled every 0.5 millimeter. Table 1 shows the results of the comparison between the DSA and CE-MRA for the two experts and the level-set based technique. The correlation coefficient indicates a better agreement between the level-set based technique and DSA than the experts. Figure 4 shows the linear regression with the 95% confidence intervals (0.89, 0.88, and 0.96 for expert I, expert II, and the level-set based method, respectively).

## 4 Discussion

A method is presented for segmentation of the ICA, which is based on level-set techniques. By using the CA as initialization, the method is better suited for segmenting vascular structures, since the initialization is everywhere near the vessel wall. The method has been applied to carotid artery stenosis grading in CE-MRA data, and compared to measurements made by clinical experts. The results show that the presented method correlates better (Spearman's correlation

coefficient 0.96 ($p<0.001$)) with DSA than the manual measurements (Spearman's correlation coefficient 0.89 and 0.88 ($p<0.001$), respectively). Also the reproducibility increased (tighter confidence bounds). Since only minimal user interaction is needed, and no restrictions are made with respect to the shape of the segmentation (*e.g.* circular cross-sections), this technique is a powerful tool in the quick and accurate determination of the degree of stenosis. Future work includes the evaluation of this technique by applying it to more patients datasets.

**Table 1.** DSA vs CE-MRA results for both experts (I and II) and the level-set based technique. Bias and 95% bounds of agreement are in units of %D.

| | Slope | %D Bias (±1.96SD) | Spearman's $r_s$ |
|---|---|---|---|
| Obs. I | 1.034 | +10.8(±30.9) | 0.89(<0.001) |
| Obs. II | 0.970 | +10.1(±30.1) | 0.88(<0.001) |
| Level-set based | 1.032 | -2.9 (±18.6) | 0.96(<0.001) |

## References

1. W.S. Moore, J.P. Mohr, H. Najafi, J.T. Robertson, R.J. Stoney, and J.F. Toole, "Carotid Endarterectomy: Practical Guidelines," *Journal of Vascular Surgery*, vol. 15, pp. 469–79, 1992.
2. North American Symptomatic Carotid Endarterectomy Trial (NASCET) Steering Committee, "NASCET. Methods, Patient Characteristics, and Progress," *Stroke*, vol. 22, pp. 711–720, 1991.
3. M.R. Patel, K.M. Kuntz, R.A. Klufas, D. Kim, and J. Kramer, "Preoperative Assessment of the Carotid Bifurcation. Can Magnetic Resonance Angiography and Duplex Ultrasonography replace Contrast Arteriography?," *Stroke*, vol. 26, pp. 1753–58, 1995.
4. E.H. Dillon, M.S. van Leeuwen, M.A. Fernandez, B.C. Eikelboom, and M. Mali, "CT Angiography: Applicationto the Evaluation of Carotid Artery Stenosis," *Radiology*, vol. 189, pp. 211–19, 1993.
5. J.J.M. Westenberg, R.J. van der Geest, M.N.J.M. Wasser, E.L. van der Linden, Th. van Walsum, A. de Roos H.C. van Assen, and J.H.C. Reiber, "Vessel Diameter Measurements in Gadolinium Contrast-Enhanced three-Dimensional MRA of Peripheral Arteries.," *Magnetic Resonance Imaging*, vol. 18, no. 1, pp. 13–22, 2000.
6. A.F. Frangi, W.J. Niessen, P.J. Nederkoorn, J. Bakker, W.P.Th. M. Mali, and M.A. Viergever, "Quantative Analysis of Vessel Morphology from 3D MR Angiograms: in Vitro and in Vivo results," *Magnetic Resonance in Medicine*, vol. 45, no. 2, pp. 311–22, 2001.
7. L.M. Lorigo, O. Faugeras, W.E.L. Grimson, R. Keriven, R. Kikinis, A. Nabavi, and C.-F. Westin, "CURVES: Curve Evolution for Vessel Segmentation," *Medical Image Analysis*, vol. 5, pp. 195–206, 2001.

8. O. Wink, W.J. Niessen, and M.A. Viergever, "Minimum Cost Path Determination Using a Simple Heuristic Function," in *Proc. International Conference on Pattern Recognition*, A. Sanfelin, J.J. Villanueva, M. Vanrell, R. Alquézar, T. Huang, and J. Serra, Eds. 2000, pp. 1010–1013, IEEE Computer Society, Piscataway, NJ.
9. A.F. Frangi, W.J. Niessen, K.L. Vincken, and M.A. Viergever, "Multiscale Vessel Enhancement Filtering," in *Proc. Medical Image Computing and Computer-Assisted Intervention*, W.M. Wells, A. Colchester, and S. Delp, Eds. 1998, Lecture Notes in Computer Science, pp. 130–137, Springer Verlag, Berlin.
10. C.M. van Bemmel, W.J. Niessen, O. Wink, B. Verdonck, and M.A. Viergever, "Blood Pool Agent CE-MRA: Improved Arterial Visualization of the Aortoiliac Vasculature in the Steady-State Using First Pass Data," in *Proc. Medical Image Computing and Computer-Assisted Intervention*, W.J. Niessen and M.A. Viergever, Eds. 2001, Lecture Notes in Computer Science, pp. 699–706, Springer Verlag, Berlin.
11. S. Osher and J.A. Sethian, "Fronts Propagating with Curvature Dependent Speed: Algorithms Based on Hamilton-Jacobi Formulations," *Journal of Computational Physics*, vol. 79, pp. 12–49, 1988.
12. J.A. Sethian, *Level Set Methods and Fast Marching Methods*, Cambridge University Press, second edition, 1999.
13. C.M. Bishop, *Neural Networks for Pattern Recognition*, Oxford University Press Inc., New York, 1995.